On the Quantification of the Bed Development Time of Alluvial Meandering Streams

Andrew D. Binns[1] and Ana Maria Ferreira da Silva, M.ASCE[2]

Abstract: This paper concerns the quantitative evaluation of the time of bed development of alluvial meandering streams. In agreement with the prevailing approach, it is assumed that the stream centerline follows a sine-generated curve; the banks are rigid. The flow is turbulent and subcritical, and the flow width is much larger than the flow depth. The movable bed is flat at time $t=0$; at $t=T_b$, the bed reaches its equilibrium or developed state. With the aid of dimensional and physical considerations, an expression is found for the duration of bed development T_b. According to this expression, T_b is proportional to the square of the flow width B and inversely proportional to the specific volumetric bed-load rate corresponding to the channel-averaged flow. The proportionality factor is found to be a function of the initial deflection angle θ_0 alone. The form of this function is investigated on the basis of a series of experimental runs carried out by the writers in a sine-generated channel having an intermediate value of θ_0 (i.e., an intermediate value of sinuosity), as well as data available in the literature.

DOI: 10.1061/(ASCE)HY.1943-7900.0000025

CE Database subject headings: Meandering streams; River beds; Topography; Evolution, development; Equilibrium; Time factors; Dimensional analysis; Laboratory tests.

Introduction

As is well known, alluvial meandering streams strive to achieve an equilibrium, or stable, state. When the flow and the stream are, either naturally or as a result of human intervention, in a nonequilibrium state, morphological changes (adjustments) occur. These include bed morphological changes as well as plan shape changes (expansion of meander loops), the bed and bank adjustments progressing with the passage of time as the stream aims to reach the equilibrium (or developed) state. The bed development process, however, is invariably considered in the literature by ignoring the bank deformation, i.e., by treating the banks as virtually rigid—an approach that is justified as the time scale of the bank deformation is usually much larger than that of the bed deformation.

Over the past 30 years or so, many theoretical and experimental studies have focused exclusively on the bed development of alluvial meandering streams. These studies extensively covered various aspects of the mechanics of bed deformation (Engelund 1974; Nelson and Smith 1989; Yalin 1992; Yalin and da Silva 2001, among many others), and detailed the nature of the deformed bed (Hooke 1974; Makaveyvev 1975; Hasegawa 1983; Whiting and Dietrich 1993a,b; Termini 1996; da Silva and El-Tahawy 2008). On the other hand, recent developments in computer hardware and software resulted in considerable progress where the simulation and prediction of bed morphological changes are concerned (Nelson and Smith 1989; Shimizu 1991; Jia and Wang 1999; Ruether and Olsen 2006, etc.). However, to date no systematic effort has been made to define the time scale of the bed development process. Consequently, it is not possible to (a priori) answer the question "What exactly will the duration of the bed development be?" Yet, as noted by Nelson and Smith (1989, p. 322) "Both the mechanism by which the channel adjusts to a perturbation from equilibrium and the time scale over which the adjustment occurs is of fundamental importance in many problems of concern to hydrologists and geomorphologists." The same, of course, applies to river engineers. Considering this, this paper is intended as the writers' contribution to the development of an expression for the quantification and prediction of the bed development time.

Following Leopold and Langbein (1966), Langbein and Leopold (1966), the centerlines of the streams (in plan view) are idealized as sine-generated curves, and therefore given by $\theta=\theta_0\cos[2\pi(l_c/L)]$, where l_c=longitudinal coordinate measured along the channel centerline from the crossover O_i [see Fig. 1(a)], L=meander length, θ=deflection angle at any l_c, and θ_0=deflection angle at $l_c=0$. It is assumed that the flow rate Q is constant, and that the flow is turbulent and subcritical; the flow width B does not vary along l_c, and is much larger than the flow depth h_{av} ($B/h_{av} > \approx 15$, say). Moreover, in agreement with the majority of current publications on the bed development process, it is also assumed that the initial surface of the movable bed is flat: its slope along the stream centerline l_c is the channel slope S_c, its slope in the radial direction being zero. An experimental "run" commences at time $t=0$. With the passage of time, the bed progressively deforms until the equilibrium (or developed) state is achieved at time $t=T_b$. The bed remains invariant for any $t \geqslant T_b$, T_b being the *duration of development* of the equilibrium bed topography, or simply, *duration of bed development*. For the sake of simplicity, the sediment transport is assumed to be by bed-load only.

[1]Ph.D. Candidate, Dept. of Civil Engineering, Queen's Univ., Kingston ON, Canada K7L 3N6. E-mail: binns@ce.queensu.ca

[2]Professor, Dept. of Civil Engineering, Queen's Univ., Kingston ON, Canada K7L 3N6 (corresponding author). E-mail: amsilva@civil.queensu.ca

Note. Discussion open until October 1, 2009. Separate discussions must be submitted for individual papers. The manuscript for this paper was submitted for review and possible publication on July 25, 2007; approved on October 25, 2008. This paper is part of the ***Journal of Hydraulic Engineering***, Vol. 135, No. 5, May 1, 2009. ©ASCE, ISSN 0733-9429/2009/5-350–360/$25.00.

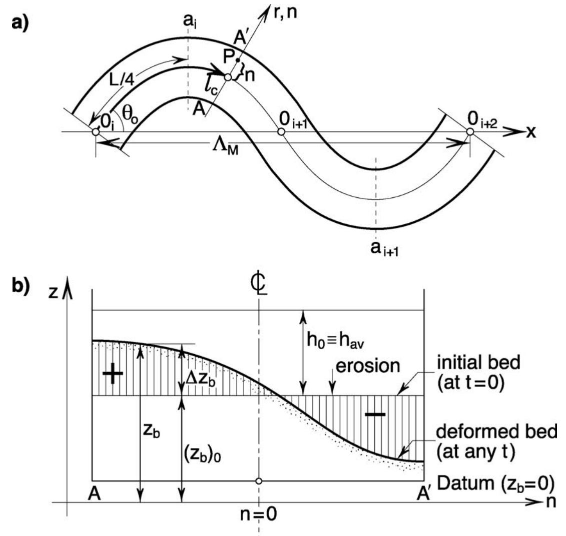

Fig. 1. Definition of variables and coordinate system: (a) plan view of stream; (b) cross section

The specific aims of this paper are:

1. To present the results of a series of experimental runs carried out by the writers in a sine-generated laboratory channel in order to reveal the duration of bed development T_b under different flow conditions; and
2. To derive (with the aid of dimensional and physical considerations) a functional relationship for T_b, and to gain some insight into the mathematical form of this relationship. For this purpose, the T_b values resulting from the present measurements will be used together with all the available data from previous experimental works.

Throughout this paper, the position of a point P in flow plan will be specified by the channel-fitted coordinates l_c and n [see Fig. 1(a)] or by their dimensionless counterparts $\xi_c = l_c/L$ and $\eta = n/B$. The difference between the local bed surface elevation z_b at any time t and the elevation of the initial flat bed surface $(z_b)_0$, will be termed Δz_b [see Fig. 1(b)].

Pertinent Aspects of the Bed Development Process under Consideration

Before proceeding further, the following pertinent aspects of the bed development process under consideration should be mentioned:

1. The bed development is entirely brought into being by the meandering of the stream—and consists of the growth, in the vertical z direction, of laterally adjacent deposition bars and erosion pools [see as examples Figs. 4(a and b) in da Silva et al. (2006), showing the developed beds measured by Losiyevskii, as reported by Makaveyvev (1975), and Jackson (1975), respectively]. Elements of bed topography due to reasons other than the meandering of the stream, namely bed forms (ripples, dunes, bars), are not considered in this work.
2. In the case of sine-generated streams, each bar+pool complex forms a large-scale erosion-deposition zone having the length $L/2$. From laboratory experiments as well as field measurements, it is known that in "wide" meandering streams the location in flow plan of the $L/2$-long erosion-deposition zones is not of a standard type, but rather dependent on the conditions in the stream (Yalin 1992; Whiting and Dietrich 1993b). More specifically, through dimensional considerations and analysis of all available data, da Silva and El-Tahawy (2008) found that the location of the erosion-deposition zones is strongly dependent on θ_0 and, to some extent, also on the ratio of meander wavelength to flow width, Λ_M/B, as well as the friction factor $(c_f)_{av}$. If θ_0 is "small" ($\theta_0 < \approx 30°$), then the upstream and downstream ends of each erosion-deposition zone are very near two consecutive apex sections (a_i and a_{i+1}, say). This implies that the most prominent erosion-deposition in any given loop occurs very near the crossover sections [for an example, see Fig. 4(a) in da Silva et al. 2006]. If θ_0 is "large" ($\theta_0 > \approx 100°$), then the upstream and downstream ends of each erosion-deposition zone are very near two consecutive crossover sections (O_i and O_{i+1}, say). In this case, the most prominent erosion-deposition in any given loop occurs very near the apex sections [for an example, see Fig. 4(b) in da Silva et al. 2006]. If θ_0 is "intermediate" ($\approx 30° < \theta_0 < \approx 100°$), then the erosion-deposition zones are situated somewhere in between the locations corresponding to small and large θ_0. For the same remaining conditions, the location of the upstream end of each $L/2$-long erosion-deposition zone gradually moves upstream from the apex a_i to the crossover O_i as θ_0 increases from small to large (for a more detailed review of the topic, see da Silva and El-Tahawy 2008).
3. Sine-generated streams consist of a (infinite) sequence of antisymmetrically identical loops conveying antisymmetrically identical flows [that is, all geometric and mechanical conditions in sections separated by half the meander wavelength $\Lambda_M/2$, such as sections O_i and O_{i+1} in Fig. 1(a), are antisymmetrically identical]. Thus, at any given instant, the sediment transport rates entering and leaving a meander loop are equal. But this means that the bed deforms with the passage of time around an unchanging average bed surface, which is the same as the flat initial bed at time $t=0$. Moreover, the field and laboratory measurements (Levi 1957; Ikeda and Nishimura 1986; Yalin and da Silva 2001) indicate that the cross-sectional areas of erosion (+ areas) and the cross-sectional areas of deposition (− areas) are (nearly) identical at any cross section and at any t, as shown in the schematic of Fig. 1(b). This, in turn, means that the channel-averaged flow depth h_{av} (see "Notation"), and thus B/h_{av}, can be regarded as constant throughout the process of bed deformation (and $h_{av} \approx h_0$). Consequently, the channel-averaged flow velocity u_{av} ($=Q/(Bh_{av})$) is also to be regarded as constant throughout the process of bed deformation (Yalin and da Silva 2001, p. 160).

Expression of Bed Development Time T_b; Dimensional and Physical Considerations

1. The phenomenon of bed development under study in this paper [the stream centerline follows a sine-generated curve; the bed shape is specified (flat) at $t=0$; the periodic flow is turbulent, subcritical and its width-to-depth ratio is "large"; the transport is by bed-load only] is fully specified by the following set of $n=10$ characteristic parameters:

$$\underbrace{\rho, \nu}_{\text{fluid}}, \quad \underbrace{D, \rho_s}_{\text{bed material}}, \quad \underbrace{\theta_0, \Lambda_M, B}_{\text{channel}}, \quad \underbrace{S_c, h_{av}, g}_{\text{flow}} \tag{1}$$

where ρ=fluid density; ν=fluid kinematic viscosity; D =typical grain size (D_{50}); ρ_s=grain density; and g =acceleration due to gravity. [Following Yalin (1972), Section 1.3 and p. 55, and in agreement with the current practice in the applications of dimensional analysis, parameters defining the shape of grains and the shape of the grain size distribution curve are omitted from Eq. (1). The reader is further referred to Yalin (1972, p. 55), for a discussion of the implications of the omission of "shape" parameters where the expressions derived from dimensional analysis are concerned.]

Since the specific weight of grains in fluid γ_s can be expressed as $\gamma_s = g(\rho_s - \rho)$, it can be used to replace g in Eq. (1); on the other hand, the shear velocity v_* $(=\sqrt{(\tau_0)_{\text{av}}/\rho})$ can be expressed as $v_* = \sqrt{gS_c h_{\text{av}}}$, and thus it can be used to replace S_c. It follows that any property A related to the phenomenon under study can be expressed as (where $v_{*\text{cr}}$=shear velocity at the critical stage)

$$A = f_A(\rho, \nu, D, \rho_s, \theta_0, \Lambda_M, B, v_*, h_{\text{av}}, \gamma_s(or\ v_{*\text{cr}})) \qquad (2)$$

2. In agreement with the current view (Hooke 1974; Nelson and Smith 1989; Struiksma and Crosato 1989; Shimizu 1991; Yalin 1992; da Silva et al. 2006, etc.), the bed deformation in "wide" meandering streams is attributed mainly to the convective behavior of the flow and thus of the sediment transport rate in the $(l_c;n)$-plane. Accordingly, the bed deformation is governed by the sediment transport continuity equation, viz

$$W = (1-p)\frac{\partial z_b}{\partial t} = -\nabla \cdot \mathbf{q}_{\text{sb}} \qquad (3)$$

where W=vertical displacement velocity of the bed surface; p=porosity of the bed material; z_b=bed elevation at time t; and $\nabla \cdot \mathbf{q}_{\text{sb}}$=(scalar) divergence of the specific volumetric bed-load rate vector $\mathbf{q}_{\text{sb}}$.

As is well known, $\mathbf{q}_{\text{sb}}$ in Eq. (3) can be evaluated from a generalized, vector form of any of the available bed-load rate equations. For the purpose of the present discussion, let us use as an example Bagnold's equation (this selection being irrelevant to the point being made below). Yalin and da Silva (2001, p. 11) have shown that, in this case, $\mathbf{q}_{\text{sb}}$ in Eq. (3) is to be evaluated with the aid of its generalized form

$$\mathbf{q}_{\text{sb}} = \bar{\mathbf{U}}[\beta'(\tau_0 - (\tau_0)_{\text{cr}})/\gamma_s] \qquad (4)$$

where $\bar{\mathbf{U}}$=vertically averaged local flow velocity vector; β' =dimensionless coefficient dependent on the properties of fluid and bed material; τ_0=magnitude of the local bed shear stress vector [$=\rho\bar{U}^2/c_f^2$; where c_f=local dimensionless (Chézy) friction factor], and $(\tau_0)_{\text{cr}}$=value of τ_0 corresponding to the initiation of sediment transport. But this means that for a specified sine-generated stream (i.e., for given values of θ_0, Λ_M, and B), the parameters ρ, ν, D, ρ_s, v_*, h_{av}, and γ_s (or $v_{*\text{cr}}$) which are necessary and sufficient to determine $\bar{\mathbf{U}}$, τ_0, and $(\tau_0)_{\text{cr}}$, are necessary and sufficient to determine also $\mathbf{q}_{\text{sb}}$ (at any instant).

3. From the explanations above, it follows that the influence of the characteristic parameters ρ, ν, D, ρ_s, v_*, h_{av}, and γ_s (or $v_{*\text{cr}}$) is completely taken into account by the bed-load rate. Considering this, and using the specific (i.e., per unit width) volumetric bed-load rate $(q_{\text{sb}})_{\text{av}}$ corresponding to the channel-averaged flow (which is *uniquely* determined by the aforementioned characteristic parameters) as the representative transport rate, one can reduce Eq. (2) to

$$A = f_A(\theta_0, \Lambda_M, B, (q_{\text{sb}})_{\text{av}}) \qquad (5)$$

This relation can be expressed in dimensionless form as

$$\Pi_A = \varphi_A(\theta_0, \Lambda_M/B) \qquad (6)$$

where Π_A=dimensionless counterpart of A.

If $A = T_b$ (where T_b=duration of bed development), then, according to Eq. (6), $\Pi_{T_b} = T_b(q_{\text{sb}})_{\text{av}}/B^2 = \varphi_T(\theta_0, \Lambda_M/B)$, which gives for T_b

$$T_b = \frac{B^2}{(q_{\text{sb}})_{\text{av}}}\varphi_T(\theta_0, \Lambda_M/B) \qquad (7)$$

4. Eq. (7) is the expression of T_b for a sine-generated stream having any arbitrary values of θ_0, Λ_M, and B. However, as is well known, the characteristic meander wavelength Λ_M of natural alluvial streams and the flow width B are not independent, but rather related by a simple proportionality: Λ_M =const$\cdot B$. According to Yalin (1992), const$\approx 2\pi$, i.e., $\Lambda_M \approx 2\pi B$. Therefore, for the streams under consideration, relation (7) reduces to

$$T_b = \frac{B^2}{(q_{\text{sb}})_{\text{av}}}\varphi_T(\theta_0) \qquad (8)$$

The function $\varphi_T(\theta_0)$ in Eq. (8) so far is an unknown function which can be revealed only with the aid of experiment. In the following sections, the writers' efforts to gain some insight into the form of this function are detailed.

Experimental Setup and Specification of Runs

The present runs were carried out in a sine-generated channel having $\theta_0 = 70°$ (i.e., a sinuosity L/Λ_M equal to 1.52). The flow width B and the meander wavelength Λ_M $(=2\pi B)$ were equal to 0.80 and 5.03 m, respectively. The channel had the total extent L_T of two meander lengths ($L_T = 2L = 15.2$ m), its first and last sections coinciding with apex sections (see Fig. 2). The upstream end of the meandering channel was connected to a 2 m long, 0.8 m wide straight approach channel. The vertical channel walls were made of 5 mm thick plywood sheets, painted with an epoxy paint. The channel bed consisted of a well-sorted silica sand having an average grain size (D_{50}) of 0.65 mm, the values of D_{16} and D_{84} being 0.42 and 0.85 mm, respectively. The specific density of the sand was 2.65.

The channel was installed in a 21 m long, 7 m wide basin equipped with a recirculating water system. The water was pumped from a sump to a constant-head reservoir, and from there it was conveyed to the channel through the system shown in Fig. 2. After its passage through the meandering channel, the water was discharged into a 9.3 m long, 2 m wide sand collection channel and then returned to the sump. A tailgate was installed at the end of the meandering channel, for the purpose of controlling the free surface slope. Further details on equipment and measurements are given elsewhere (Binns 2006).

In total, five runs were carried out. In each run, the flow rate Q was constant. All runs started from a flat bed having zero radial slope and a specified longitudinal slope S_c (flat initial bed at $t = 0$). The bed was subsequently allowed to deform under the action of the flow until a time t substantially beyond the stage where, visually, the bed in the channel reach under consideration

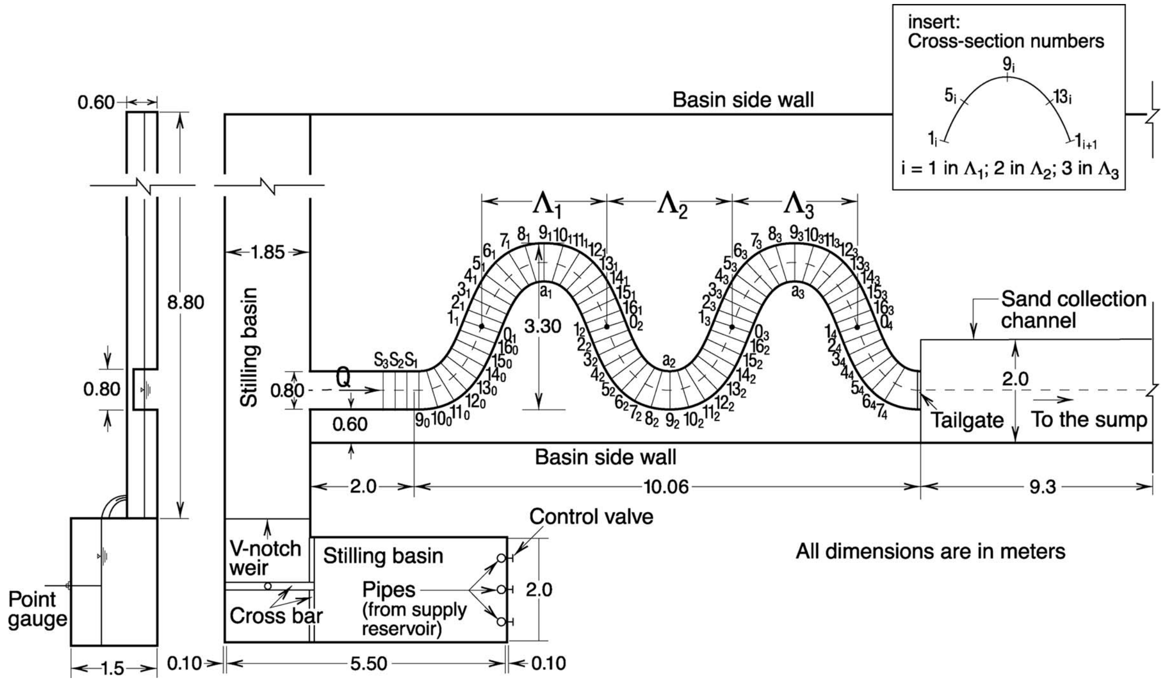

Fig. 2. Schematic of experimental facility

(see the next section) appeared to have achieved its equilibrium state. At the beginning of the runs, the free surface elevation at the downstream end of the meandering channel was set so that the free surface slope S_f along the channel centerline (assumed to be representative of the channel-averaged free surface slope) was identical to the slope of the flat initial bed S_c ("uniform" flow conditions). Small adjustments to the position of the tailgate were occasionally required during the runs in order to maintain $S_f \approx S_c$. The channel-averaged flow depth h_{av} was identified with the (identical) flow depth h_0 at the centerline of the four consecutive crossovers 1_1, 1_2, 1_3, and 1_4 [see the section on "Pertinent Aspects of the Bed Development Process under Consideration," paragraph (3)]. The flow depth h_0 at the centerline of each crossover was obtained as the difference between the free surface elevation measured immediately after the "uniform" flow conditions were established and the elevation of the surface of the flat initial bed $(z_b)_0$. To avoid interference with the natural bed development, no sediment was fed to the channel throughout the runs. For the present runs, this procedure did not compromise the intended analysis (see second and third paragraphs of the next section).

In order to monitor the bed development with the passage of time, the runs were stopped at regular time intervals to allow measurements of the bed surface elevation z_b. In stopping and restarting the runs, care was taken not to disturb the bed. Upon restarting, the flow conditions were observed to very quickly become reinstated, or at least very nearly so. Thus the effect of stopping and restarting the runs on the estimates of the duration of bed development presented later on, is judged to be small, although owing to this reason alone these estimates may be somewhat systematically underestimated. The measurements of the bed surface elevation z_b were carried out at 66 equally spaced cross sections (see Fig. 2). Note that in each of the three consecutive meander loops in the channel, Λ_1, Λ_2, and Λ_3, the 16 equally spaced measurement cross sections were numbered 1_i to 16_i, the subscript i (=1, 2 or 3) marking the loop (Λ_1, Λ_2, or Λ_3) to which the cross section belongs. The distance along the channel centerline between any two adjacent measurement cross sections was equal to 23.8 cm. In each cross section the bed surface elevation was measured at 22 equally spaced points, from $n=-36.75$ to 36.75 cm (i.e., from $\eta \approx -0.46$ to 0.46). For this purpose, a device formed by 22 vertical rods installed on a horizontal bar resting on the (leveled) top of the channel walls was used. Each rod was individually lowered until the pointer on the rod touched the bed surface. All bed surface elevation measurements were carried out by using as reference level (datum) a horizontal plane located 30 cm below the top of the channel walls. The sediment retained in the sand collection channel at the end of each time step was collected and measured volumetrically. This corresponded to bed-load transport, as in the present runs the material moved as bed-load only.

The hydraulic conditions of the runs are summarized in Table 1. In addition to the values of quantities defined earlier, Table 1 also displays the values of the following channel-averaged quantities: $(c_f)_{\mathrm{av}}$=dimensionless (Chézy) friction factor [evaluated as $2.5\ln(0.368(h_{\mathrm{av}}/k_s))+B_s$, where $k_s \approx 2D_{50}$ (Kamphuis 1974) is the granular roughness of the bed surface and B_s is the roughness function, determined in this paper from Eq. (1.10) in Yalin and da Silva (2001)], R=flow Reynolds number, F=Froude number, R_*=roughness Reynolds number, Y/Y_{cr}=relative flow intensity (where Y=mobility number and Y_{cr}=value of Y at the stage of initiation of sediment transport), and $(q_{\mathrm{sb}})_{\mathrm{av}}$=channel-averaged specific volumetric bed-load rate (see "Notation" for definition of quantities above). For the present sand, Y_{cr} was identified with 0.031. The values of $(q_{\mathrm{sb}})_{\mathrm{av}}$ were obtained on the basis of the sand collected from the sand collection channel after the formation of the bar-pool complexes had been accomplished—so as to ensure that the reported $(q_{\mathrm{sb}})_{\mathrm{av}}$ values were not distorted by local transfers of bed material associated with the formation of the bar-pool complexes.

As can be seen from Table 1, the values of h_{av} were similar in all runs, their average value being 4.38 cm; the bed slope S_c was

Table 1. Summary of Hydraulic Conditions in Present Experimental Runs ($\theta_0=70°$; $B=0.80$ m; $D=0.65$ mm)

Run	Q (m^3/s)	h_{av} (cm)	S_c	u_{av} (m/s)	v_* (m/s)	B/h_{av}	$(c_f)_{av}$	R	F	R_*	Y/Y_{cr}	$(q_{sb})_{av}$ [a] (m^2/s)
1	0.0070	4.55	1/400	0.193	0.033	17.6	15.3	8,763	0.29	43	3.42	5.95×10^{-6}
2	0.0095	4.14	1/250	0.286	0.040	19.3	14.9	11,838	0.45	52	4.97	1.25×10^{-5}
3	0.0106	4.43	1/200	0.298	0.047	18.1	15.0	13,200	0.45	61	6.65	1.90×10^{-5}
4	0.0122	4.34	1/150	0.352	0.053	18.4	14.9	15,288	0.54	69	8.69	3.20×10^{-5}
5	0.0138	4.45	1/125	0.387	0.059	18.0	15.0	17,238	0.59	77	10.69	4.30×10^{-5}

[a]Values of $(q_{sb})_{av}$ listed are measured values.

increased from 1/400 in Run 1 to 1/125 in Run 5. Consequently, in the present runs the values of Y/Y_{cr} increased from 3.42 in Run 1 to 10.69 in Run 5, and the values of $(q_{sb})_{av}$ increased from 5.95×10^{-6} m^2/s in Run 1 to 4.30×10^{-5} m^2/s in Run 5; the values of B/h_{av} and $(c_f)_{av}$ can be regarded as fixed ($B/h_{av}\approx18.3$ and $(c_f)_{av}\approx15$). The flow was in the transitional regime of turbulent flow ($\approx5<\mathsf{R}_*\leqslant\approx70$) in Runs 1–4, and in the rough turbulent regime ($\mathsf{R}_*>\approx70$) in Run 5.

The total duration of the runs was 180 min for Runs 1 and 2, 120 min for Run 3, and 75 min for Runs 4 and 5, respectively. The times at which the runs were stopped and bed surface elevation measurements were carried out are given in Table 2.

Experimental Observations and Results

Using the bed surface elevation measurements, bed elevation contour plots, and bed longitudinal profiles were produced for all measurement times. As examples, the bed elevation contour plots corresponding to Run 2 ($S_c=1/250$) at $t=10$ and 75 min are shown in Figs. 3(a and b), respectively; those corresponding to Run 4 ($S_c=1/150$) at $t=5$ and 30 min are shown in Figs. 4(a and b), respectively. These plots were produced from the measured Δz_b values ($\Delta z_b>0$ implying deposition, and $\Delta z_b<0$, erosion). Figs. 5 and 6 also show as examples the longitudinal bed profiles corresponding to $n=26.25$ cm (i.e., $\eta=0.3281$) at different measurement times of Runs 2 and 4, respectively. In these figures, $\xi_c=0$ corresponds to cross section 1_1 (see Fig. 2). [To help visualize the location of the bed profiles, note that the point P in Fig. 1(a) is located at $\eta\approx0.3281$.]

As a result of not feeding sand at the channel entrance, the flow picked up sand from the upstream end of the experimental channel (both from the straight approach channel as well as the curved part immediately downstream) as needed to compensate for the lack of feeding. The amount of bed degradation due to this process as well as the channel stretch affected by it increased with the passage of time. This is illustrated in Fig. 7, showing as an example the plots of cross-sectional average bed surface elevation $(z_b)_{cs}$ versus ξ_c corresponding to Run 4 at $t=5$ and 30 min. Indeed, in the left-hand side of these plots $(z_b)_{cs}$ is seen to deviate more and more from the elevation of the flat initial bed as time passes during a run. The deviation of $(z_b)_{cs}$ from the elevation of the flat initial bed is further exaggerated as the flow in all runs (as exemplified by Figs. 3 and 4) formed a pool at the inner bank around the first crossover of loop Λ_1 (the material eroded from this pool being deposited immediately downstream to form the bar situated around the apex of the same loop). Moreover, the formation of the bar at the outer bank around the aforementioned crossover was largely impeded because of the breakup of channel periodicity at the channel entrance (the required upstream pool that would act as the primary source of sediment for this bar could not form).

From the $(z_b)_{cs}$ plots of all runs, it was estimated that the region affected by degradation had extended approximately to the apex section of the first meander loop Λ_1 (i.e., to cross section 9_1 at $\xi_c=0.25$) by the time the bed at the downstream reaches had achieved its developed or equilibrium state (see the next section, and in particular Table 3 for the values of the related equilibrium times). Therefore, the conditions can be regarded as periodic, or at least very nearly so, and thus representative of those under study in this work (see the section entitled "Pertinent Aspects of the Bed Development Process under Consideration") only in the region of the channel approximately downstream of the apex of loop Λ_1, where $\xi_c=0.25$. As mentioned earlier, the existence of periodic conditions implies that the same pattern of bar-pool complex repeats itself throughout the loops (which was observed for $\xi_c>\approx0.25$ in the contour plots of all runs, as exemplified by Figs. 3 and 4). It also implies equality of sediment transport rates entering and leaving the loops as reflected by a bed that deforms around an unchanging average bed surface coinciding with the flat initial bed (which was also observed for $\xi_c>\approx0.25$ in all runs, as exemplified by Fig. 7 corresponding to Run 4 [note how in this figure $(z_b)_{cs}$ tends to follow $(z_b)_0$ once $\xi_c>\approx0.25$].

As can be inferred from Figs. 3–6, the bed deformation (consisting of the growth of laterally adjacent bars and pools) progressed very rapidly during the early stages of each run, and then gradually slowed down with the passage of time.

The location in flow plan of the bars and pools (i.e., of the $L/2$ long erosion-deposition zones) was identical in all five runs, irrespective of their value of Y/Y_{cr}. The beginnings and ends of each

Table 2. Measurement Times of Bed Surface Elevation ($t=0$ at Beginning of Runs)

Run	Measurement times (min)											
1	10	20	30	40	50	60	75	90	105	120	150	180
2	10	20	30	40	50	60	75	90	105	120	150	180
3	6	12	18	24	30	40	50	60	75	90	105	120
4	5	10	15	20	25	30	35	40	50	60	75	—
5	4	8	12	16	20	30	40	50	60	75	—	—

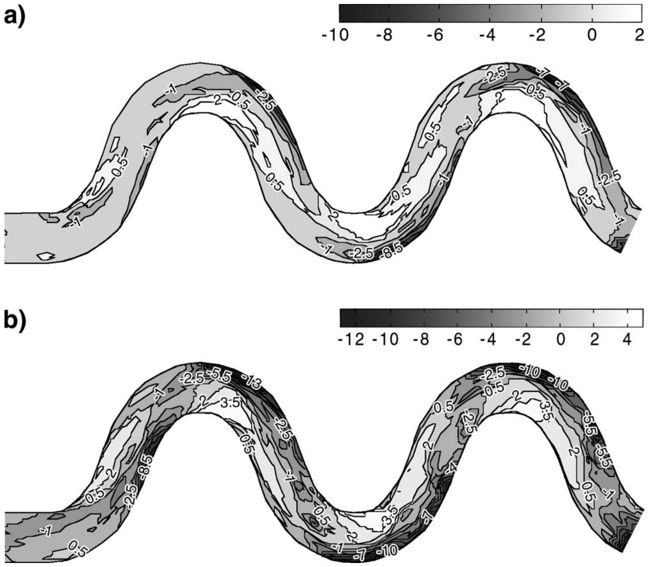

Fig. 3. Bed elevation contour-plots for Run 2, $S_c=1/250$ (contours based on Δz_b values; units are cm; flow from left to right): (a) at $t=10$ min; (b) at $t=75$ min

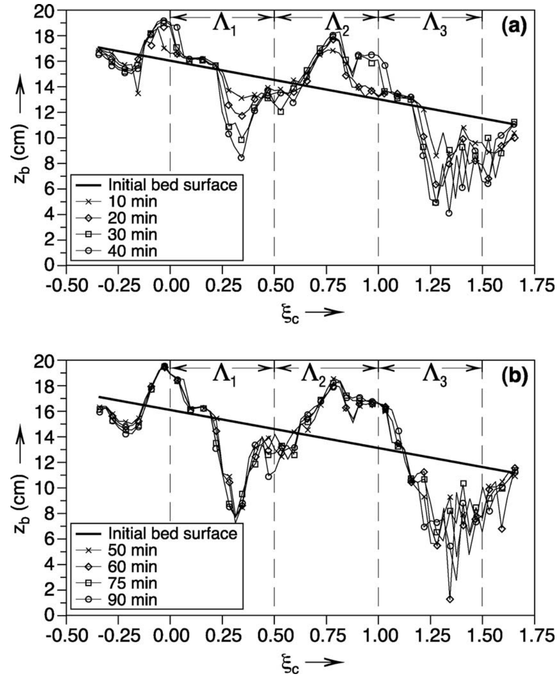

Fig. 5. Longitudinal bed profiles corresponding to $\eta=0.3281$ for Run 2 ($S_c=1/250$): (a) at $t=10$, 20, 30, and 40 min; (b) at $t=50$, 60, 75, and 90 min

erosion-deposition zone in the present runs coincided approximately with cross sections 5_i and 5_{i+1} ($i=1,2,3$; see Fig. 2)—as indicated by the bed elevation contour plots of Runs 2 and 4 shown in Figs. 3 and 4, respectively. Both of these observations are consistent with the findings by da Silva and El-Tahawy (2008) (see earlier section on "Pertinent Aspects of the Bed Development Process under Consideration," paragraph 2).

Bed forms such as dunes and ripples did not occur in Run 1. However, dunes were observed in Runs 2 to 5. The length and height of the dunes varied (increased) throughout the runs as the dunes evolved to a developed stage, the dune height also varying (increasing) with the flow depth in the pools. However, the dunes acquired some prominence only at the later stages of the runs, particularly in Runs 4 and 5 (having the largest values of Y/Y_{cr}). But even then the occurrence of dunes that could be viewed as significant from the bed roughness standpoint was restricted to a small region strictly around the deepest locations of the pools. The effect of dunes on the flow, if any, was minor and can be disregarded.

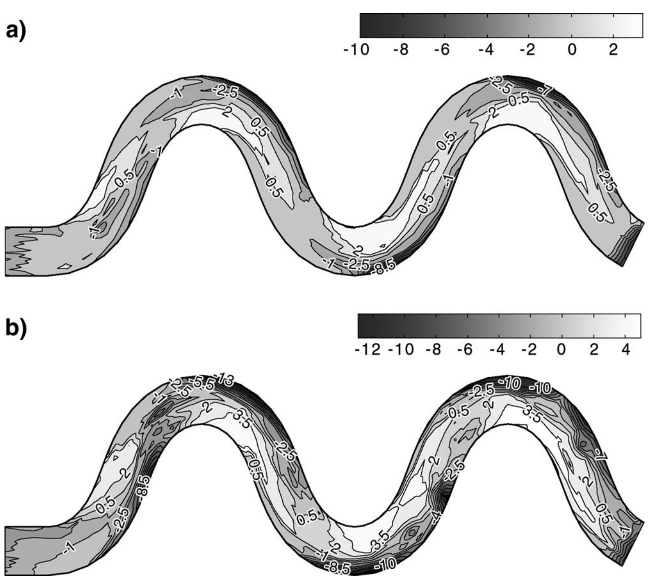

Fig. 4. Bed elevation contour plots for Run 4, $S_c=1/150$ (contours based on Δz_b values; units are cm; flow from left to right): (a) at $t=5$ min; (b) at $t=30$ min

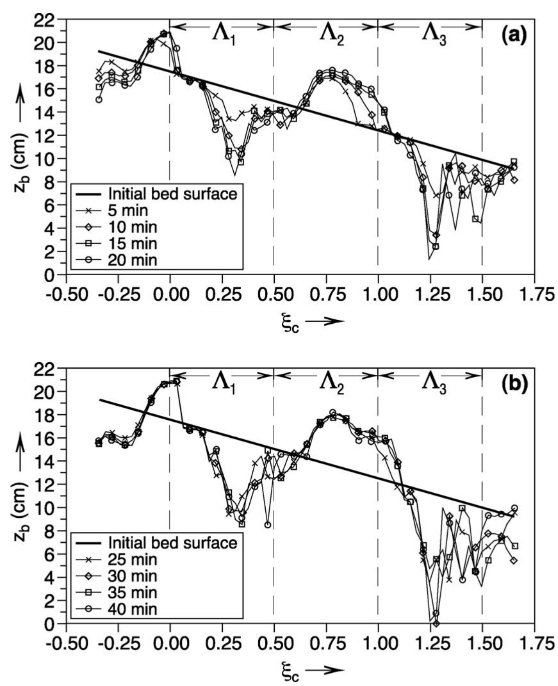

Fig. 6. Longitudinal bed profiles corresponding to $\eta=0.3281$ for Run 4 ($S_c=1/150$): (a) at $t=5$, 10, 15, and 20 min; (b) at $t=25$, 30, 35, and 40 min

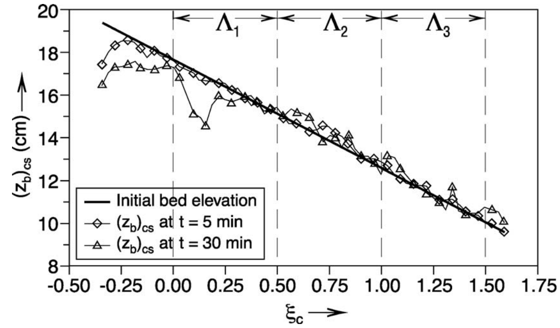

Fig. 7. Plots of cross-sectional average bed surface elevation $(z_b)_{cs}$ versus ξ_c for Run 4 ($S_c=1/150$) at $t=0$, 5, and 30 min

The only effect of increasing the slope and thus the sediment transport capacity in the present runs was to increase the rate of development of the bed. The equilibrium bed topographies produced in each of the five runs were similar in nature: not only, as mentioned earlier, were the locations of the erosion-deposition zones identical, but the magnitudes of maximum erosion and deposition were also similar. To illustrate this point, consider Figs. 3 and 4, and observe how similar the bed geometry at $t=10$ min of Run 2 ($S_c=1/250$) is to that at $t=5$ min of Run 4 ($S_c=1/150$); and how similar the bed geometry at $t=75$ min of Run 2 is to that at $t=30$ min of Run 4.

Determination of Duration of Bed Development T_b

In this work, the duration of bed development T_b is determined on the basis of the differences between longitudinal bed profiles at consecutive measurement times. Use is made of the fact that these differences tend to zero as equilibrium is approached. Since the time between consecutive measurements was increased toward the end of the runs (see Table 2), the differences per unit time were considered. Only the second $L/2$-long erosion-deposition zone (falling within $\approx 0.625 \leqslant \xi_c \leqslant \approx 1.125$) was used in the determination of T_b. This region was selected because, as follows from the previous section, the bed development in it was unaffected by the lack of feeding as well as the breakup of channel periodicity at the channel entrance. Moreover, in contrast to the third $L/2$-long erosion-deposition zone (falling within $\approx 1.125 \leqslant \xi_c \leqslant \approx 1.625$), the selected zone is sufficiently far from the downstream end of the channel so that it can also be regarded as unaffected by any possible exit effects.

For any given value of $\eta(=n/B)$ within the region $\approx 0.625 \leqslant \xi_c \leqslant \approx 1.125$, let $\mathcal{D}_\eta$ be the sum of absolute differences between the ordinates z_b of the longitudinal bed profiles corresponding to any two consecutive measurement times t_{i+1} and t_i, divided by $t_{i+1}-t_i$

$$\mathcal{D}_\eta = \frac{\sum_{\xi_c=0.625}^{1.125} \left|(z_b)_{t_{i+1}} - (z_b)_{t_i}\right|}{t_{i+1}-t_i} \tag{9}$$

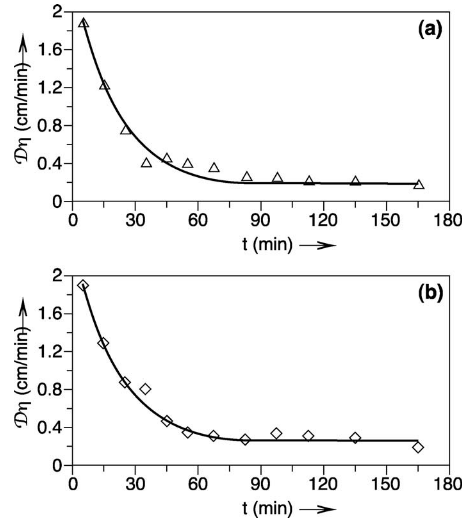

Fig. 8. Plots of $\mathcal{D}_\eta$ versus time for Run 2 ($S_c=1/250$): (a) plot corresponding to $\eta=0.1969$; (b) plot corresponding to $\eta=0.3281$

In order to determine the duration of bed development T_b, plots of $\mathcal{D}_\eta$ versus time were produced for all values of η at which bed elevation measurements were taken. As examples, the plots of $\mathcal{D}_\eta$ versus time corresponding to $\eta=0.1969$ and 0.3281 for Run 2 ($S_c=1/250$) are shown in Figs. 8(a and b), respectively.

For each plot of $\mathcal{D}_\eta$ versus time, the duration of bed development was identified with the time at which $\mathcal{D}_\eta$ became zero or reduced to a constant residual value. For each run this yielded various estimates of the duration of bed development, with average values as shown in Table 3. The standard deviations of these estimates were 7.9, 5.6, 5.3, 2.7, and 3.9 min for Runs 1 to 5, respectively. In the following, the values of T_b for each of the present runs will be identified with the corresponding average values in Table 3.

Substitution into Eq. (8) of these values of T_b, together with $B=0.80$ m and the measured values of $(q_{sb})_{av}$ (see Table 1), yielded the five estimates of $\varphi_T(\theta_0=70°)$ shown in Table 3. In the following, $\varphi_T(\theta_0=70°)$ will be identified with the average value of these five estimates, namely 0.086.

Observe that by using $B=0.80$ m and $\varphi_T(\theta_0=70°)=0.086$ in Eq. (8), one obtains the following equation:

$$T_b = \frac{0.0551}{(q_{sb})_{av}} \tag{10}$$

which expresses the dependency of T_b with $(q_{sb})_{av}$ for the specific values of B and θ_0 of the present experimental runs. The graph of Eq. (10) is shown, together with the data points representing the present runs, in Fig. 9.

Table 3. Values of T_b and $\varphi_T(\theta_0)$ in Present Runs

Run	T_b (min)	$\varphi_T(\theta_0)$
1	108	0.060
2	82	0.096
3	46	0.082
4	29	0.087
5	26	0.105
Average:		0.086

Variation of $\varphi_T(\theta_0)$ with θ_0

From the present experiments, one value of the not yet known function $\varphi_T(\theta_0)$ has emerged, namely that corresponding to θ_0

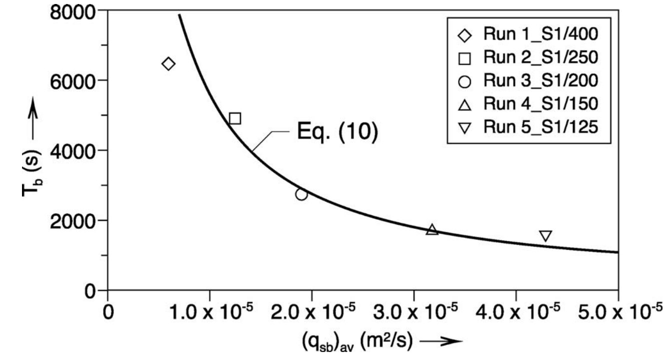

Fig. 9. Plot of T_b versus $(q_{sb})_{av}$ for conditions of present runs (B =0.80 m; θ_0=70°)

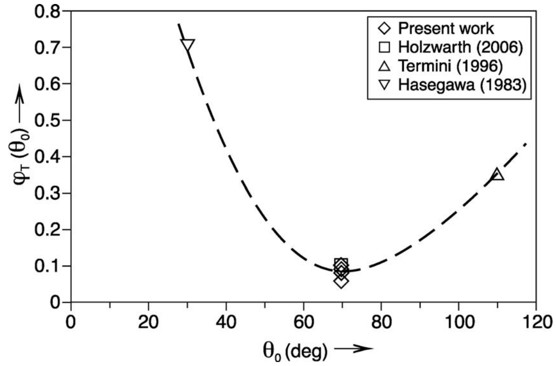

Fig. 10. Plot of experimental values of $\varphi_T(\theta_0)$ versus θ_0

=70°. In order to fully reveal the nature of the function $\varphi_T(\theta_0)$, several further "points" of this function, corresponding to different values of θ_0, are needed. Yet, despite the fact that several authors in the past conducted experiments in sine-generated channels where they allowed the flat initial bed to deform until the equilibrium state was reached, estimates of the time of development T_b were provided only by Hasegawa (1983) for his Run ME-2 in a 30° channel (also see Shimizu and Itakura 1989), Holzwarth (2006) for one run in the present 70° channel, Whiting and Dietrich (1993b) for their Run 100-3 (θ_0=100°), and Termini (1996) for one run in a 110° channel. In the run carried out by Whiting and Dietrich (1993b), large-scale bars ("shingle" bars) scaling with the flow width were superimposed on the bar-pool complexes brought into being by meandering of the stream. As a result, the bed exhibited not just one pool per meander loop, but also superimposed on this rather prominent pools spaced at approximately 3–4 times the flow width. It is not possible to discern whether the reported time of equilibrium corresponds to the formation of the shingle bars or of the bar-pool complex attributable to the meandering of the stream—nor is it known to what extent the two processes occurring simultaneously interfere with each other and their individual times of development. For this reason, the run by Whiting and Dietrich (1993b) will not be considered in the analysis presented below.

The hydraulic conditions of the remaining runs and the estimates of T_b given by their authors are shown in Table 4. Since Hasegawa (1983) and Termini (1996) did not report bed-load rate measurements, the values of $(q_{sb})_{av}$ corresponding to their runs in Table 4 are calculated values, obtained with the aid of Bagnold's bed-load equation. As is well-known, this equation can be expressed as $(q_{sb})_{av}=(\gamma_s^{1/2}D^{3/2}/\rho^{1/2})\cdot(B_s\beta)\cdot Y^{1/2}(Y-Y_{cr})$ (see Yalin 1972, 1992). For the bed materials of the two runs under consideration and water, $\beta\approx 0.425$ (Yalin 1972), γ_s=16,186.5 N/m^3 and ρ=1,000 kg/m^3; B_s and Y_{cr} were determined to be 9.24 and 0.032, respectively, for the run by Hasegawa (1983), and 8.90 and 0.031 for the run by Termini (1996).

Substituting the values of B, T_b, and $(q_{sb})_{av}$ for each of the aforementioned runs into Eq. (8), one obtains the estimates of $\varphi_T(\theta_0)$ shown in the last column of Table 4. These values are plotted versus θ_0, together with those obtained for the present runs, in Fig. 10. The data points in this figure suggest that $\varphi_T(\theta_0)$ first decreases as θ_0 increases, reaches a minimum somewhere around $\theta_0\approx 70°$, and then gradually increases as θ_0 increases. This result is analyzed in paragraphs (1) and (2) below in light of the sediment transport continuity equation and the nature of convective behavior of flow in sine-generated streams. Before proceeding further, however, it seems in order to point out the following. Estimates of $(q_{sb})_{av}$ for the runs by Hasegawa (1983) and Termini (1996) were also obtained with the aid of Yalin, van Rijn, and Meyer-Peter bed-load equations [selected as a means to characterize well-known discrepancies in estimates of $(q_{sb})_{av}$ by different equations/approaches]. The values of $(q_{sb})_{av}$ given by Yalin, van Rijn, and Meyer-Peter equations were 1.37, 1.82, and 1.75 times larger, respectively, than that given by Bagnold's equation for the run by Hasegawa (1983); and 1.28, 1.54, and 1.77 times larger, respectively, for the run by Termini (1996). Since $\varphi_T(\theta_0)\sim(q_{sb})_{av}$ [see Eq. (8)], if the bed-load equations by Yalin, van Rijn, or Meyer-Peter would have been used to estimate $(q_{sb})_{av}$ instead of Bagnold's equation, then the points representing the runs by Hasegawa (1983) and Termini (1996) in the $(\varphi_T(\theta_0);\theta_0)$-plan in Fig. 10 would be situated higher than shown in the figure. The aforementioned trend of the data, however, would not be altered (it would, in fact, become only more exaggerated). It should also be noted that there is some evidence that the value of $(q_{sb})_{av}$ in the run by Hasegawa (1983) should be much nearer to the lowest estimate provided by Bagnold's equation than to the higher estimate provided by Meyer-Peter equation. Indeed, Shimizu and Itakura (1989), who numerically calculated the bed deformation for the run by Hasegawa (1983) using Meyer-Peter equation reported that: "in the computations it took 100 min to reach the equilibrium state…The difference in time to reach the equilibrium state between the experiment

Table 4. Hydraulic Conditions of Experimental Runs by Previous Authors

Author	Run	θ_0 (degrees)	Λ_M/B	D (mm)	B (m)	Q (l/s)	h_{av} (cm)	S_c	R	F	R_*	Y/Y_{cr}	$(q_{sb})_{av}$ (m²/s)	T_b (min)	$\varphi_T(\theta_0)$
Hasegawa (1983)[a]	ME-2	30	6.8	0.43	0.30	1.87	2.60	0.0322	6,233	0.47	25	3.79	4.42×10^{-6}	240	0.707
Holzwarth (2006)[b]	1	70	2π	0.65	0.80	6.21	2.40	0.0080	7,763	0.67	56	5.77	1.56×10^{-5}	70	0.103
Termini (1996)[a]	—	110	2π	0.65	0.50	6.50	3.00	0.0037	13,000	0.80	43	3.33	5.88×10^{-6}	250	0.353

[a]Values of $(q_{sb})_{av}$ for runs are estimated with the aid of Bagnold's equation.

[b]Values of $(q_{sb})_{av}$ for run is a measured value.

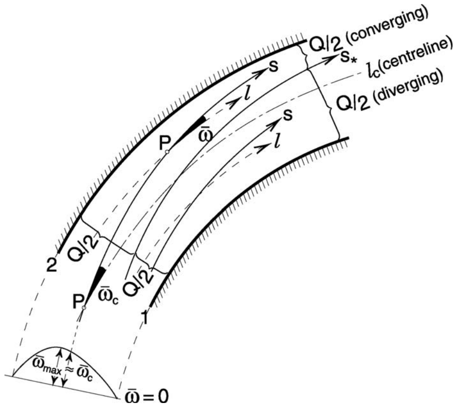

Fig. 11. Laterally adjacent convergence-divergence flow zones in meandering flow (after da Silva et al. 2006)

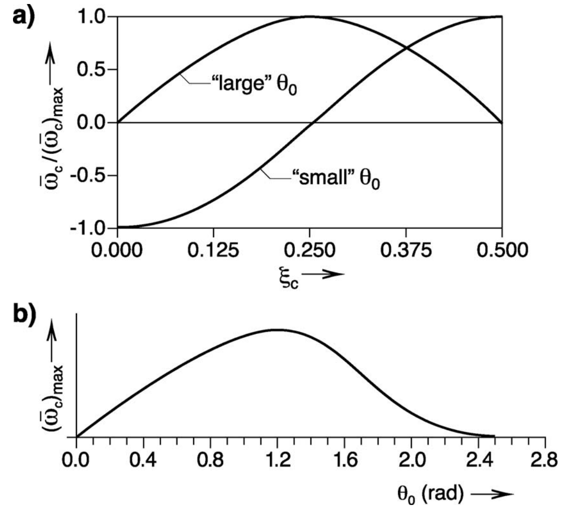

Fig. 12. Descriptors of convective behavior of meandering flow (schematic representations): (a) $\bar{\omega}_c$-curves [normalized by $(\bar{\omega}_c)_{\max}$] showing variation of $\bar{\omega}_c$ along ξ_c for channels having "small" and "large" values of θ_0; (b) variation of $(\bar{\omega}_c)_{\max}$ with θ_0

(240 min) and the calculations (100 min) can be reduced by introducing a more appropriate bed-load transport formula." Thus, despite the fact that the value of $\varphi_T(\theta_0)$ in Table 4 for the run by Hasegawa is but an estimate based on the adoption of Bagnold's equation, this value is likely to be realistic. No similar information is available for the run by Termini (1996)—the considerations above suggesting that the corresponding value of $\varphi_T(\theta_0)$ in Table 4 may be underestimated.

1. From both flow measurements and numerical simulations (Engelund 1974; Smith and McLean 1984; Nelson and Smith 1989; Shimizu and Itakura 1989; Yalin 1992; da Silva et al. 2006, etc.), it is known that the vertically-averaged flow in meandering channels is formed by laterally adjacent converging (convectively accelerating) and diverging (convectively decelerating) flow zones (see the schematic in Fig. 11). In the case of sine-generated streams, the convergence-divergence zones of flow have the length $L/2$ and periodically alternate along l_c.

   Since the local sediment transport rate $\mathbf{q}_{sb}$ is an increasing function of the (local) vertically-averaged flow velocity $\bar{\mathbf{U}}$ [see Eq. (4)], the convective variation of $\bar{\mathbf{U}}$ in a flow zone must inevitably cause the corresponding convective variation of $\mathbf{q}_{sb}$ in that zone; i.e., it must cause the scalar $\nabla\cdot\mathbf{q}_{sb}$ to acquire a nonzero value. According to the sediment transport continuity equation [Eq. (3)], if the flow is convectively accelerating, i.e., if $\nabla\cdot\mathbf{q}_{sb}>0$, then erosion occurs ($W<0$), and if the flow is convectively decelerating, i.e., if $\nabla\cdot\mathbf{q}_{sb}<0$, then deposition occurs ($W>0$).

   Let us now integrate Eq. (3) along $0<t<T_b$. This yields

$$(1-p)(z_b)_T = -\int_0^{T_b} \nabla\cdot\mathbf{q}_{sb}\,dt = -(\nabla\cdot\mathbf{q}_{sb})_m T_b = W_m T_b \tag{11}$$

   i.e.

$$T_b = -(1-p)\frac{(z_b)_T}{(\nabla\cdot\mathbf{q}_{sb})_m} = (1-p)\frac{(z_b)_T}{W_m} \tag{12}$$

   This relation conveys that the duration of development of the bed surface at a location of flow plan is a decreasing function of $-(\nabla\cdot\mathbf{q}_{sb})_m = W_m$, and thus of the "intensity" of the convergence-divergence of flow at that location.

2. Let $\bar{\omega}$ be the local vertically-averaged deviation angle, i.e., the angle between the vertically-averaged streamlines s and the coordinate lines l of a meandering flow; and $\bar{\omega}_c$ be the value of $\bar{\omega}$ at the channel centerline. In a sine-generated channel, the cross-sectional distribution of $\bar{\omega}$ is as shown in Fig. 11: $\bar{\omega}=0$ at the banks, the largest cross-sectional values of $\bar{\omega}$ occurring in the neighborhood of the channel centerline (Hasegawa 1983; Nelson and Smith 1989; Yalin and da Silva 2001). Clearly, at the cross sections coinciding with the upstream and downstream ends of each $L/2$-long convergence-divergence zone of flow, $\bar{\omega}_c=0$. The sign of $\bar{\omega}$, and thus the sign of $\bar{\omega}_c$, remains the same (positive or negative) within each $L/2$-long zone, and therefore it alternates periodically along ξ_c. As first pointed out by Yalin (1992), this means that the $\bar{\omega}_c$-curve, showing how $\bar{\omega}_c$ varies along ξ_c, fully reflects the location in flow plan of the $L/2$-long convergence-divergence zones of a given flow. [This is illustrated in the schematic in Fig. 12(a), drawn following da Silva et al. (2006), and showing the distinctly different $\bar{\omega}_c$-curves (normalized by the maximum value of $\bar{\omega}_c$ along ξ_c, $(\bar{\omega}_c)_{\max}$) corresponding to flows in channels having "small" and "large" values of θ_0. (In the case of "small" θ_0, the upstream and downstream ends of the $L/2$-long laterally adjacent convergence-divergence zones of flow coincide approximately with consecutive apexes; in the case of "large" θ_0, with consecutive crossovers.)]

Clearly, the maximum value of $\bar{\omega}_c$ along ξ_c [i.e., $(\bar{\omega}_c)_{\max}$] is a measure of the "intensity" of the convergence-divergence of flow. da Silva et al. (2006) have observed that, with all other determining parameters remaining the same, $(\bar{\omega}_c)_{\max}$ varies with θ_0 as shown in the schematic of Fig. 12(b). Observe that $(\bar{\omega}_c)_{\max}$ increases as the deviation of θ_0 from $\approx 70°$ (1.22 rad) decreases. But if so, and if as shown in paragraph (1) above, T_b and thus $\varphi_T(\theta_0)$, vary inversely with the "intensity" of flow [and consequently with $(\bar{\omega}_c)_{\max}$], then $\varphi_T(\theta_0)$ must be expected to decrease as the deviation of θ_0 from $\approx 70°$ decreases. This is consistent with the trend of the data in Fig. 10, as indicated by the dashed line in this figure.

Conclusions

The main results of this work can be summarized as follows:

1. The duration of development T_b of the equilibrium bed topography in alluvial meandering streams has been found to be proportional to the square of the flow width B and inversely proportional to the specific volumetric bed-load rate $(q_{sb})_{av}$ corresponding to the channel-averaged flow [Eq. (8)], the proportionality factor $\varphi_T(\theta_0)$ being a function of the initial deflection angle θ_0 alone.
2. On the basis of the five experimental runs carried out by the writers in a sine-generated channel having $\theta_0=70°$, it has been found that $\varphi_T(\theta_0=70°)=0.086$.
3. The location in flow plan of the $L/2$ long erosion-deposition zones was identical in the present experimental runs, irrespective of their value of Y/Y_{cr}. This is consistent with Yalin (1992), Whiting and Dietrich (1993b), and da Silva and El-Tahawy (2008), from where it follows that the location of erosion-deposition zones in "wide" meandering streams should be dependent only on θ_0, Λ_M/B, and $(c_f)_{av}$.
4. The only effect of increasing Y/Y_{cr} (and thus the sediment transport capacity) in the present runs was to increase the rate of bed development. The "height" of bed deformation at equilibrium was similar in all five runs (irrespective of their value of Y/Y_{cr}). This is in contrast to the height of bed forms (dunes and ripples) which, as is well known, is strongly dependent on Y/Y_{cr}.
5. Fig. 10—where the values of $\varphi_T(\theta_0)$ from the runs carried out by previous authors in channels having "small" and "large" values of θ_0 are plotted together with those resulting from the present runs—suggests that the function $\varphi_T(\theta_0)$ first decreases as θ_0 increases, reaches a minimum somewhere around $\theta_0 \approx 70°$, and then gradually increases as θ_0 increases. This result is consistent with known aspects of the nature of convective behavior of flow and bed deformation as presented in the previous section.
6. The present work cannot be viewed but as a first step toward the determination of the function $\varphi_T(\theta_0)$ (and thus the quantification of T_b)—for even if some insight has been gained into the form of variation of $\varphi_T(\theta_0)$, the establishment of the exact expression of this function is, at present, clearly hindered by the scarcity of pertinent data. This work thus highlights the need for further experimental tests involving the systematic variation of θ_0 and the measurement of all pertinent variables (including $(q_{sb})_{av}$), and directed toward determination of the expression of $\varphi_T(\theta_0)$. Future research is also needed to address the eventual generalization of the present work to the more complicated conditions present in natural streams.

Acknowledgments

This research was supported by the Natural Sciences and Engineering Research Council of Canada (NSERC) through a Discovery Grant provided to the second writer. The writers are grateful to two anonymous reviewers, whose valuable suggestions were of great help in developing this manuscript to its present form.

Notation

The following symbols are used in this paper:

B = flow width;
c_f = dimensionless (Chézy) friction factor;
D = representative grain size ($=D_{50}$);
D_η = sum of absolute differences between ordinates z_b of longitudinal bed profiles at times t_{i+1} and t_i, as defined by Eq. (9);
F = Froude number ($=u_{av}/\sqrt{gh_{av}}$);
g = acceleration due to gravity;
h_{av} = channel-averaged flow depth (averaged over an integer number of meander cycles or half cycles);
k_s = granular roughness of bed surface ($k_s \approx 2D_{50}$);
L = meander length (measured along l_c);
l_c = longitudinal coordinate along centerline of meandering flow; $l_c=0$ at crossover O_i [see Fig. 1(a)];
n = radial coordinate of meandering flow; $n=0$ at flow centerline [see Fig. 1(a)];
p = porosity of bed material;
Q = flow rate;
q_{sb} = magnitude of specific (i.e., per unit width) volumetric local bed-load rate vector $\mathbf{q}_{sb}$;
$(q_{sb})_{av}$ = specific (i.e., per unit width) volumetric bed-load rate corresponding to channel-averaged flow;
R_* = roughness Reynolds number ($=v_* k_s/\nu$);
S_c = bed slope along centerline of meandering flow;
T_b = duration of development of the equilibrium (or stable) bed topography;
t = time;
$\overline{U}$ = magnitude of vertically-averaged local flow velocity vector $\overline{\mathbf{U}}$;
u_{av} = channel-averaged flow velocity (averaged over an integer number of meander cycles or half cycles);
v_* = channel-averaged shear velocity ($=\sqrt{(\tau_0)_{av}/\rho}=\sqrt{gh_{av}S_c}$);
W = vertical displacement velocity of bed surface;
Y = mobility number [$=(\tau_0)_{av}/(\gamma_s D)=\rho v_*^2/(\gamma_s D)$];
z_b = bed elevation measured with regard to an arbitrary reference datum;
γ_s = specific weight of grains in fluid [$=g(\rho_s-\rho)$];
Δz_b = difference between local elevation of deformed bed surface and elevation of initial flat bed surface at $t=0$ [$\Delta z_b=z_b-(z_b)_0$];
θ, θ_0 = deflection angle of meandering flow at any l_c and at $l_c=0$, respectively;
Λ_M = meander wavelength;
ν = fluid kinematic viscosity;
ξ_c, η = dimensionless counterparts of l_c and n, respectively ($\xi_c=l_c/L$ and $\eta=n/B$);
Π_A = dimensionless counterpart of quantity A;
ρ = fluid density;
ρ_s = grain density;
τ_0 = local bed shear stress;
$(\tau_0)_{av}$ = channel-averaged bed shear stress (averaged over an integer number of meander cycles or half cycles);
ϕ_A = dimensionless function determining the dimensionless version Π_A of a property A;

ϕ_T = dimensionless function determining the dimensionless version Π_T of duration of bed development T_b;

$\overline{\omega}$ = local vertically-averaged deviation angle (angle between vertically-averaged streamline s and coordinate line l of meandering flow); and

$\overline{\omega}_c$ = value of $\overline{\omega}$ at centerline of meandering flow.

Subscripts

cr = marks the value of a quantity corresponding to initiation of sediment transport (to the "critical stage");

cs = marks the cross-sectional average value of a quantity;

m = marks the value of a quantity integrated over $0 < t < T_b$;

T = marks the value of a quantity at time $t = T_b$; and

0 = marks the value of a quantity at $t = 0$; exceptions are τ_0 and θ_0.

References

Binns, A. D. (2006). "Time-evolution and stability of the bed in sine-generated meandering streams: An experimental study." MSc thesis, Queen's Univ., Kingston, Canada.

da Silva, A. M. F., and El-Tahawy, T. (2008). "On the location in flow plan of erosion-deposition zones in sine-generated meandering streams." *J. Hydraul. Res.*, 46(1), 49–60.

da Silva, A. M. F., El-Tahawy, T., and Tape, W. D. (2006). "Variation of flow pattern with sinuosity in sine-generated meandering streams." *J. Hydraul. Eng.*, 132(10), 1003–1014.

Engelund, F. (1974). "Flow and bed topography in channel bends." *J. Hydr. Div.*, 100(11), 1631–1648.

Hasegawa, K. (1983). "Hydraulic research on planimetric forms, bed topographies and flow in alluvial rivers." Ph. D. thesis, Hokkaido Univ., Sapporo, Japan (in Japanese).

Holzwarth, S. (2006). "Bed deformation in sine-generated meandering streams having large values of the width-to-depth ratio." Diplomarbeit thesis, Technische Univ. Hamburg, Harburg, Germany, and Queen's Univ., Kingston, Canada.

Hooke, R. L. (1974). "Distribution of sediment transport and shear stress in a meander bend." *Rep. No. 30*, Uppsala Univ. Naturgeografiska Inst., Uppsala, Sweden.

Ikeda, S., and Nishimura, T. (1986). "Flow and bed profile in meandering sand-silt rivers." *J. Hydraul. Eng.*, 112(7), 562–579.

Jackson, R. J. (1975). "Velocity-bed-form-texture patterns of meander bends in the lower Wabash River of Illinois and Indiana." *Geol. Soc. Am. Bull.*, 86(11), 1511–1522.

Jia, Y., and Wang, S. S. Y. (1999). "Numerical model for channel flow and morphological change studies." *J. Hydraul. Eng.*, 125(9), 924–933.

Kamphuis, J. W. (1974). "Determination of sand roughness for fixed beds." *J. Hydraul. Res.*, 12(2), 193–203.

Langbein, W. B., and Leopold, L. B. (1966). "River meanders—Theory of minimum variance." *U.S. Geol. Surv. Prof. Pap.*, 422-H, 1–15.

Leopold, L. B., and Langbein, W. B. (1966). "River meanders." *Sci. Am.*, 214(6), 60–70.

Levi, I. I. (1957). *Dynamics of alluvial streams*, State Energy Publishing, Leningrad, Russia (in Russian).

Makaveyvev, N. I. (1975). *River bed and erosion in its basin*, Press of the Academy of Sciences of the USSR, Moscow.

Nelson, J. M., and Smith, J. D. (1989). "Evolution and stability of erodible channel beds." *River meandering*, S. Ikeda, and G. Parker, eds., Vol. 12, Water Resource Monograph, American Geophysical Union, Washington, D.C., 321–378.

Ruether, N., and Olsen, N. R. B. (2006). "3D modeling of transient bed deformation in a sine-generated channel with two different width to depth ratios." *Proc., 3rd Int. Conf. River Flow 2006*, Ferreira, Alves, Leal & Cardoso, eds., Taylor & Francis Group, London, 1269–1275.

Shimizu, Y. (1991). *A study on prediction of flows and bed deformation in alluvial streams*, Civ. Eng. Res. Inst., Hokkaido Development Bureau, Sapporo, Japan (in Japanese).

Shimizu, Y., and Itakura, T. (1989). "Calculation of bed variation in alluvial channels." *J. Hydraul. Eng.*, 115(3), 367–384.

Smith, J. D., and McLean, S. R. (1984). "A model for flow in meandering streams." *Water Resour. Res.*, 20(9), 1301–1315.

Struiksma, N., and Crosato, A. (1989). "Analysis of a 2-D bed topography model for rivers." *River meandering*, S. Ikeda, and G. Parker, eds., Vol. 12, Water Resour. Monograph, American Geophysical Union, Washington, D.C., 153–180.

Termini, D. (1996). "Evolution of a meandering channel with an initial flat bed: Theoretical and experimental study of the channel bed and the initial kinematic characteristics of flow." Ph.D. thesis, Univ. of Palermo, Palermo, Italy (in Italian).

Whiting, P. J., and Dietrich, W. E. (1993a). "Experimental constraints on bar migration through bends: Implications for meander wavelength selection." *Water Resour. Res.*, 29(4), 1091–1102.

Whiting, P. J., and Dietrich, W. E. (1993b). "Experimental studies of bed topography and flow patterns in large-amplitude meanders. 1. Observations." *Water Resour. Res.*, 29(11), 3605–3614.

Yalin, M. S., and da Silva, A. M. F. (2001). *Fluvial processes*, IAHR Monograph, IAHR, Delft, The Netherlands.

Yalin, M. S. (1972). *Mechanics of sediment transport*, Pergamon, Oxford, U.K.

Yalin, M. S. (1992). *River mechanics*, Pergamon, Oxford, U.K.